Supporting Information

NIR light-triggered drug delivery system using core-shell gold nanostars-mesoporous silica nanoparticles by multiphoton absorption photo-dissociation of 2-nitrobenzyl PEG

Andy Hernández Montoto,[1,2] Mónica Gorbe,[1,2,3] Antoni Llopis-Lorente,[1,2] José Manuel Terrés,[1] Roberto Montes,[1] Roberto Cao-Milán,[4] Borja Díaz de Greñu,[1,2] María Alfonso,[1,2] Mar Orzaez,[3,5] María Dolores Marcos,[1,2,3,6] Ramón Martínez-Máñez,*[1,2,3,6] Félix Sancenón[1,2,3,6]

[1] Instituto Interuniversitario de Investigación de Reconocimiento Molecular y Desarrollo Tecnológico, Universitat Politècnica de València, Universitat de València. E-mail: rmaez@qim.upv.es

[2] CIBER de Bioingeniería, Biomateriales y Nanomedicina (CIBER-BBN).

[3] Unidad Mixta UPV-CIPF de Investigación en Mecanismos de Enfermedades y Nanomedicina. Universitat Politècnica de València-Centro de Investigación Príncipe Felipe, Valencia, Spain.

[4] Facultad de Química, Universidad de La Habana, 10400 La Habana, Cuba.

[5] Centro de Investigación Príncipe Felipe, Laboratorio de Péptidos y Proteínas, Carrer d'Eduardo Primo Yúfera, 3, 46012 València, Spain.

[6] Departamento de Química, Universitat Politècnica de València, Camino de Vera s/n, 46022 Valencia, Spain.

Materials and Methods

Chemicals: Tetrachloroauric acid aqueous solution 30%, polyvinylpyrrolidone (PVP, Mw=10000), hexadecyltrimethylammonium bromide (CTAB), tetraethoxysilane (TEOS), ammonia aqueous solution 32%, ammonium nitrate, (3-aminopropyl) triethoxysilane (APTES), vanillin, ethyl bromoacetate, sodium carbonate, nitric acid 70%, acetic anhydride, hydrochloric acid 36 %, sodium hydroxide, sodium borohydride, sodium chloride, sodium sulphate anhydrous, triethylamine, *N*-(3-dimethylaminopropyl)-*N*'-ethylcarbodiimide hydrochloride (EDC), 1-hydroxibenzotriazole monohydrate (HOBt), succinic anhydride, 4-dimethylaminopiridine (DMAP), *N*-hydroxysuccinimide (NHS) and methoxypolyethyleneglycol amine (PEG-NH_2, Mw=800) were purchased from Aldrich. Doxorubicin hydrochloride (Dox) was purchased from Carbosynth Limited. Analytical grade solvents were purchased from Scharlau. HeLa cells were purchased from the German Resource Center for Biological Materials. Dulbecco´s Modified Eagle Medium (DMEM), Fetal Bovine Serum (FBS), Dulbecco´s Phosphate Buffer Saline (PBS), trypsin, Hoechst 33342 and cell proliferation reagent WST-1 were purchased from Sigma-Aldrich.

Instrumentation: The reaction progress was monitored on precoated silica gel TLC Al foils Sigma-Aldrich with fluorescent indicator 254 nm (60 A medium pore diameter). Spots were visualized under 254 nm UV light. ^{1}H and ^{13}C NMR spectra were respectively recorded at 400 MHz and 100 MHz on a Bruker 400 Avance III instrument. Chemical shifts (δ) are reported in parts per million (ppm) from low to high field and referenced to residual solvent. Coupling constants (J) are reported in hertz (Hz). Standard abbreviations indicating multiplicity are used as follows: s = singlet, d = doublet, t = triplet, q = quartet, m = multiplet. Fourier transform infrared (FT-IR)

spectra were recorded using a Bruker TENSOR27 spectrometer. Transmission electron microscopy (TEM) images were collected using a JEOL JEM-1010 microscope operating at 100 kV. Optical extinction spectra were recorded using a JASCO V-650 UV/vis spectrophotometer. Fluorescence spectroscopy was carried out on a JASCO FP-8300 spectrofluorometer (Hitachi High Technologies). X-ray measurements were performed on a Bruker AXS D8 Advance diffractometer using Cu-Kα radiation. Thermo-gravimetric analyses were carried out on a TGA/SDTA 851e Mettler Toledo equipment, using an oxidant atmosphere (Air, 80 mL min^{-1}) with a heating program consisting on a heating step from 298 K to 373 K at heating rate of 10 K min^{-1}, then an isothermal heating step at 373 K during 30 minutes, a third heating step from 373 K to 1273 K at heating rate of 10 K min^{-1} and finally an isothermal heating step at 1273 K during 30 minutes. N_2 adsorption-desorption isotherms were recorded on a Micromeritics ASAP2010 automated sorption analyzer. The samples were degassed at 120 ºC under vacuum overnight. The specific surface areas were calculated from the adsorption data in the low pressures range using the Brunauer-Emmett-Teller (BET) method. Pore size was determined by following the Barrett−Joyner−Halenda (BJH) model. Hydrodynamic diameter and zeta potential measurements were performed by dynamic light scattering using a Malvern Zeta sizer Nano ZS instrument.

Synthesis

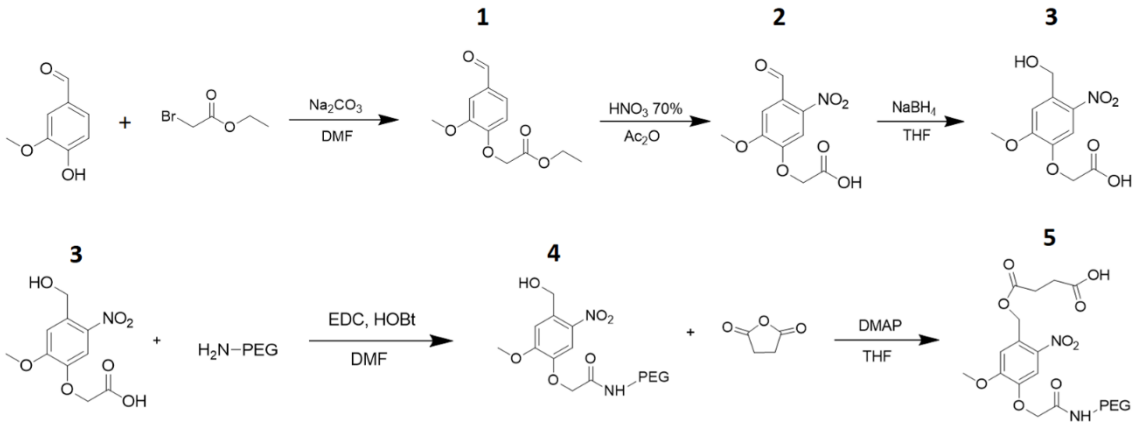

Scheme S1. Synthesis of photolabile PEG derivative **5** bearing a 2-nitrobenzyl linker.

Synthesis of compound 1: A mixture of vanillin (2.5 g, 16 mmol), ethyl bromoacetate (2 mL, 3 g, 18 mmol) and sodium carbonate (3.5 g, 25 mmol) in DMF (15 mL) was stirred at room temperature for 24 h. Water was added, and the mixture was partitioned between ethyl acetate and saturated NaCl solution. The organic phase was dried with anhydrous Na_2SO_4 and evaporated to yield the aldehyde-ester **1** (3.5 g, 15 mmol, 90 % yield) as a white solid (Scheme S1). ^{1}H-NMR (400 MHz, $CDCl_3$) δ 9.83 (s, 1H), 7.41 (d, J=1.9, 1H), 7.39 (dd, J=8.1, 1.9, 1H), 6.86 (d, J=8.1, 1H), 4.75 (s, 2H), 4.24 (q, J=7.1, 2H), 3.92 (s,3H),1.26 (t, J=7.1,3H); ^{13}C-NMR (100 MHz, $CDCl_3$) δ 190.9, 168.1, 152.6, 150.1, 131.2, 126.2, 112.5, 110.0, 66.0, 61.7, 56.1, 14.2.

Synthesis of compound 2: A solution of aldehyde-ester **1** (3.5 g, 15 mmol) in acetic anhydride (10 mL) was added to a cooled solution of 70 % HNO_3 (10 mL) and acetic anhydride (15 mL) at 0 ºC. The resultant mixture was stirred for 2 h and then allowed to warm to room temperature and stirring was continued for an additional 4 h. The reaction mixture was poured into a cold water, the pH adjusted with solid NaOH to 13-

14 and then with 36 % HCl to 2-3. The aqueous phase was extracted with EtOAc and the organic phase dried and evaporated to yield a yellow solid. Recrystallization from MeOH/H_2O afforded the product nitro-acid **2** (3 g, 12 mmol, 80 % yield) (Scheme S1). ^{1}H-NMR (400 MHz, $CDCl_3$) δ 10.24 (s, 1H), 7.40 (s, 1H), 7.24 (s, 1H), 4.66 (s, 2H), 3.86 (s, 3H); ^{13}C-NMR (100 MHz, $CDCl_3$) δ 187.4, 168.9, 153.3, 150.4, 143.1, 126.0, 110.1, 108.7, 65.6, 56.5.

Synthesis of compound 3: To a solution of nitro-acid **2** (1 g, 4 mmol) in THF (20 mL) $NaBH_4$ (0.5 g, 13 mmol) was added at room temperature. The reaction mixture was stirred for 24 h. Water was added and the pH adjusted with HCl (1 M) to 2-3. The aqueous phase was extracted with EtOAc and the organic phase dried and evaporated to yield a pale yellow solid **3** (0.95 g, 3.7 mmol, 95 % yield) (Scheme S1). ^{1}H-NMR (400 MHz, $CO(CD_3)_2$) δ 7.73 (s, 1H), 7.54 (s, 1H), 4.99 (s, 2H), 4.87 (s, 2H), 4.00 (s, 3H); ^{13}C-NMR (100 MHz, $CO(CD_3)_2$) δ 169.8, 155.4, 146.8, 139.7, 136.0, 111.5, 111.2, 66.5, 61.8, 56.7.

Synthesis of compound 4: A mixture of compound **3** (0.125 g, 0.5 mmol), PEG-NH_2 (0.4 g, 0.54 mmol), HOBt (0.075 g, 0.55 mmol), EDC (0.1 g, 0.52 mmol) and Et_3N (0.075 mL, 0.055 g, 0.54 mmol) in DMF (5 mL) was stirred for 24 h at room temperature. The reaction mixture was partitioned between ethyl acetate and saturated NaCl solution. The organic phase was dried and evaporated to yield solid **4** (0.35 g, 0.35 mmol, 71 % yield) (Scheme S1). ^{1}H-NMR (400 MHz, $CO(CD_3)_2$) δ 7.79 (s, 1H), 7.59 (s, 1H), 4.99 (s, 2H), 4.63 (s, 2H), 4.04 (s, 3H), 3.68-3.52 (m, 68H), 3.29 (s, 3H); ^{13}C-NMR (100 MHz, $CO(CD_3)_2$) δ 168.0, 155.5, 146.5, 136.6, 126.0, 112.4, 111.2, 72.63, 71.2 (x29), 71.0 (x2), 70.2, 70.0, 61.6, 58.8, 56.9, 39.4.

Synthesis of compound 5: A mixture of alcohol **4** (0.24 g, 0.24 mmol), succinic anhydride (0.03 g, 0.3 mmol) and DMAP (0.035 g, 0.3 mmol) in THF (5 mL) was

stirred for 24 h at room temperature. Water was added, and the pH adjusted with HCl (1 M) to 2-3. The aqueous phase was extracted with EtOAc and the organic phase dried and evaporated to yield a solid **5** (0.16 g, 0.15 mmol, 63 % yield) (Scheme S1). ^{1}H-NMR (400 MHz, $CO(CD_3)_2$) δ 7.82 (s, 1H), 7.28 (s, 1H), 5.51 (s, 2H), 4.66 (s, 2H), 4.06 (s, 3H), 3.68-3.52 (m, 68H), 3.29 (s, 3H), 2.75 (m, 2H), 2.68 (m, 2H); ^{13}C-NMR (100 MHz, $CO(CD_3)_2$) δ 173.8, 172.6, 168.0, 155.4, 147.3, 129.6, 126.0, 112.5, 111.7, 72.6, 71.2 (x29), 71.0 (x2), 70.2, 69.8, 63.5, 58.8, 57.2, 39.5, 30.6, 30.5.

Synthesis of gold nanostars (AuNSts): Gold nanostars were synthesized by seeded growth method using PVP solution in DMF. At 25 ºC, 50 µL of an aqueous solution of 166 mM $HAuCl_4$ was mixed with 15 mL of 20 mM PVP solution in DMF. After 5 min, 10 µL of preformed seed dispersion (15 nm gold nanospheres coated with PVP in ethanol, c(Au) = 6.5 mM) was added and allowed to react for 24 h without stirring. Gold nanoparticles were recovered by centrifugation (20 min, 9500 rpm) and washed five times with water by centrifugation and redispersion. The concentration of Au in all gold colloids was derived from their extinction spectra (absorbance at 400 nm).

Synthesis of gold nanostars coated with mesoporous silica shell (AuNSt@mSiO$_2$-NH$_2$): Briefly, 50 mL of a 6.6 mM aqueous CTAB solution was mixed with 20 mL of ethanol at 25 ºC in a 250 mL round bottom flask under magnetic stirring (400 rpm). Ar gas was bubbled into solution for 1 h and inert atmosphere was kept during the synthesis. Once the solution was transparent and free of bubbles, 50 µL of ammonia aqueous solution 32% was added. Subsequently, 3 mL of AuNSt dispersion (c(Au) = 5 mM) was poured into the synthesis solution. After 5 min, 40 µL of TEOS was added dropwise. The mixture was stirred for 15 min, and then 10 µl of APTES was added. After 24 h the particles were recovered (10 min, 9500 rpm) and washed twice in ethanol. Finally, the CTAB template was removed by extraction process dispersing

nanoparticles in 50 mL NH_4NO_3 solution in ethanol (10 mg/mL). The mixture was stirred for 8 hours and particles were recovered by centrifugation. This extraction process was repeated three times in order to achieve the removal of higher amount of CTAB from mesoporous channels.

Synthesis of N2 nanoparticles: The amino functionalized AuNSt@mSiO_2-NH_2 nanoparticles (2 mg) were dispersed in 1.5 ml of Dox in ethanol (1 mg/ml) and stirred for 18 h. Dox-loaded nanoparticles were recovered by centrifugation and re-dispersed in 1.5 ml of compound **5** in THF, previously activated with EDC and NHS. Then, the mixture was stirred for 18 h at 25 ºC. The nanoparticles were recovered by centrifugation, washed with THF and H_2O and finally dried.

Cargo photo-release experiments

A well in the 96-well plate was filled with 250 μL of nanoparticles suspensions. The NIR laser-triggered drug release experiments were performed with a laser diode (808 nm) that was set at 1 cm above the liquid surface. The sample volume was irradiated at a predetermined power density (1 W cm^{-2}). Also, a control sample was kept in the dark. At a predetermined interval upon NIR irradiation, the samples were centrifuged (3 min, 9500 rpm) and the fluorescence spectra of supernatants at 595 nm (λ_{exc} = 490 nm) were recorded.

Cell viability and internalization assays

HeLa cells were grown at 37 ºC under humidified air containing CO_2 (5% vol.) in Dulbecco's Modified Eagle Medium (DMEM), which was supplemented with fetal bovine serum (10% vol. FBS, Gibco), penicillin/streptomycin (1% vol., 10000 units of

both per mL). After 24 h of incubation, cells were rinsed with PBS, and then detached with trypsin (0.2% vol.)/PBS. The HeLa cells were seeded in 96-well plates with a density of 5.0 x 10^3 cells per well and grown in DMEM for another 24 h. The cells were then treated with the nanoparticle suspensions in DMEM at different concentrations. Then the designated cells were exposed to a NIR laser irradiation (808 nm, 1 W cm^{-2}, 10 min). Upon the switching-off of the laser, the treated cells were incubated for another 48 h. After the incubation period, the cells were rinsed with PBS, and the cell viabilities were evaluated via the WST-1 assay. Typically, cell proliferation reagent WST-1 (7 μL) was added, and then the cells were incubated for another 1 h at 37 ºC. The absorbance at 450 nm was measured using a micro-plate reader (Perkin Elmer Wallac 1420 Victor2). Percentage of cell viabilities were determined relative to the untreated cells (control, 100 % viability). Three replicates were done for each treatment groups.

For NIR light triggered delivery of Dox using confocal laser scanning microscopy (CLSM), cells were seeded in 96 well plate with glass bottom at a density of 5.0 x10^3 cells per well and grown in DMEM for 24 h. Cells were incubated with **N2** nanoparticles at 50 μg mL^{-1} for 2 h. Then, the designated cells were irradiated with 808 nm laser at 1 W cm^{-2} for 15 min and were incubated for another 2 h. Then, cells were rinsed with PBS, and freshly DMEM was added. Finally, DNA marker Hoechst 33342 (2 μg mL^{-1}) was added, and cells were incubated for 5 min before CLSM analysis. CLSM images were recorded using a Leica TCS SP8 (Leica Microsystems CMS GmbH) confocal laser scanning microscope. Also, intracellular Dox release was tested by *in situ* irradiation of nanoparticles in cells at 633 nm using the laser of microscope. CLSM images were taken before and after the irradiation period.

Cell internalization of nanoparticles was tested by transmission electron microscopy (TEM). TEM images were acquired using a microscope FEI Tecnai Spirit G2 operating

at 80 kV with a digital camera (Soft Image System, Morada). Hela cells were incubated with nanoparticle suspension in DMEM at 30 µg mL^{-1} during 24 h. Then, cells were fixed with glutaraldehyde (3%) in sodium phosphate buffer (0.1 $mol \cdot L^{-1}$), dehydrated in ethanol and stained with osmium tetroxide (1%) and uranyl acetate (1%). Finally, the samples were embedded in epoxy resin (Araldite) and sectioned for analysis.

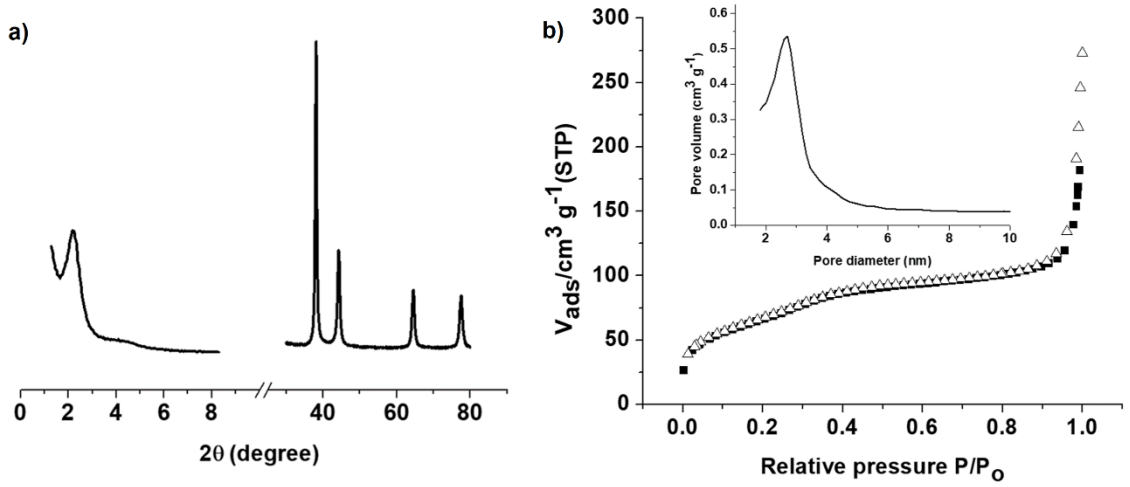

Figure S1. (a) PXRD patterns and (b) N_2 adsorption-desorption isotherms of AuNSt@mSiO_2-NH_2 nanoparticles (inset: pore size distribution).

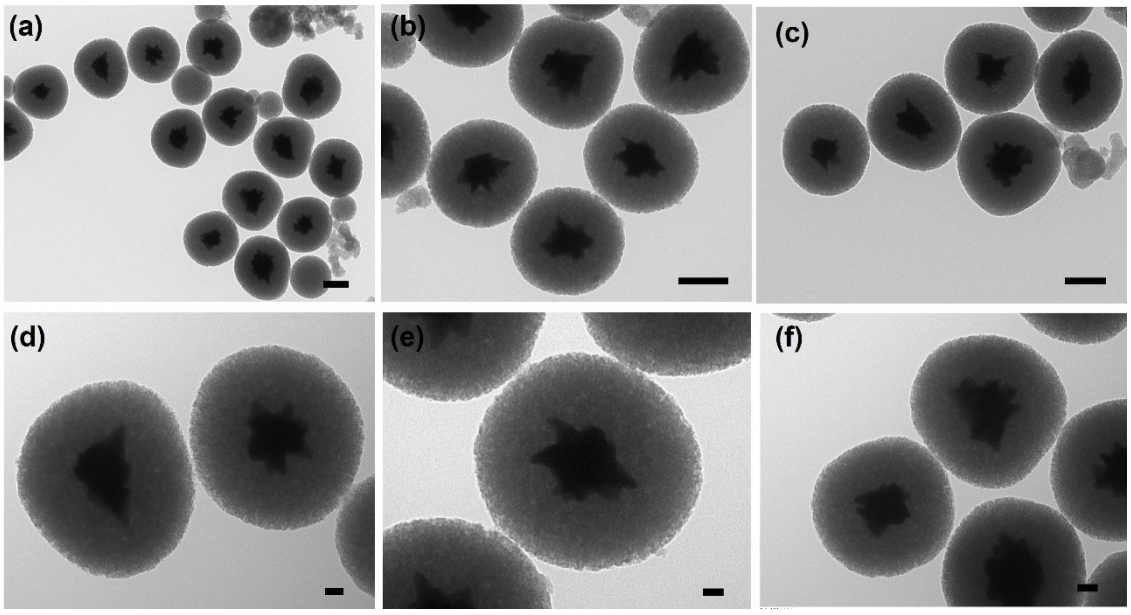

Figure S2. TEM images of **N2** nanoparticles. Scale bar: (a,b,c) 100 nm, (d,e,f) 20 nm.

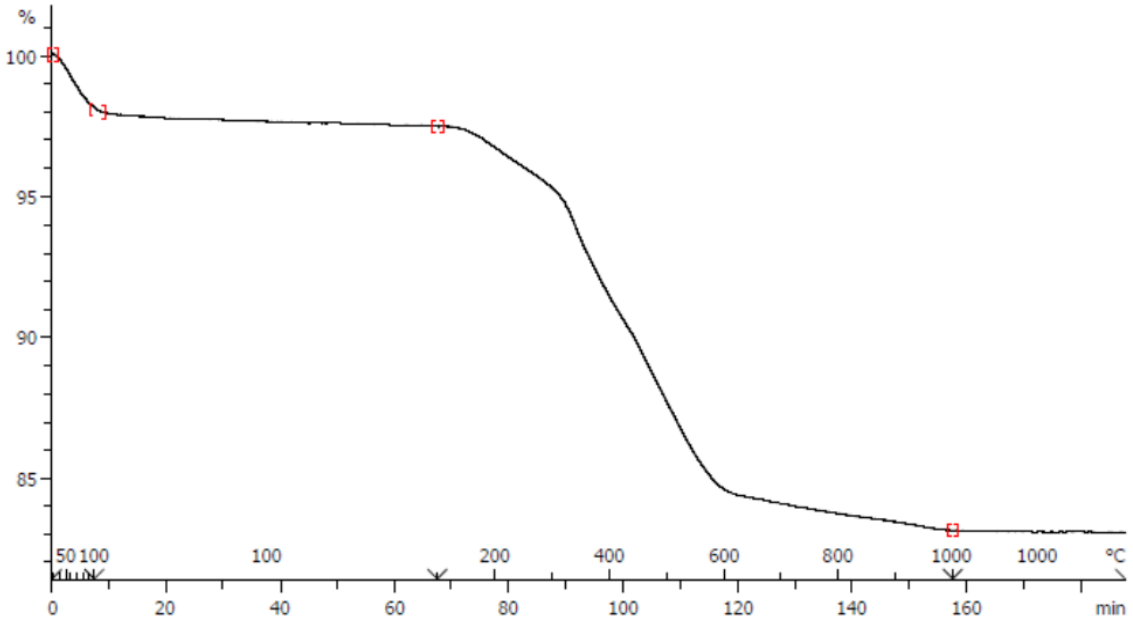

Figure S3. TGA trace of **N2** nanoparticles.

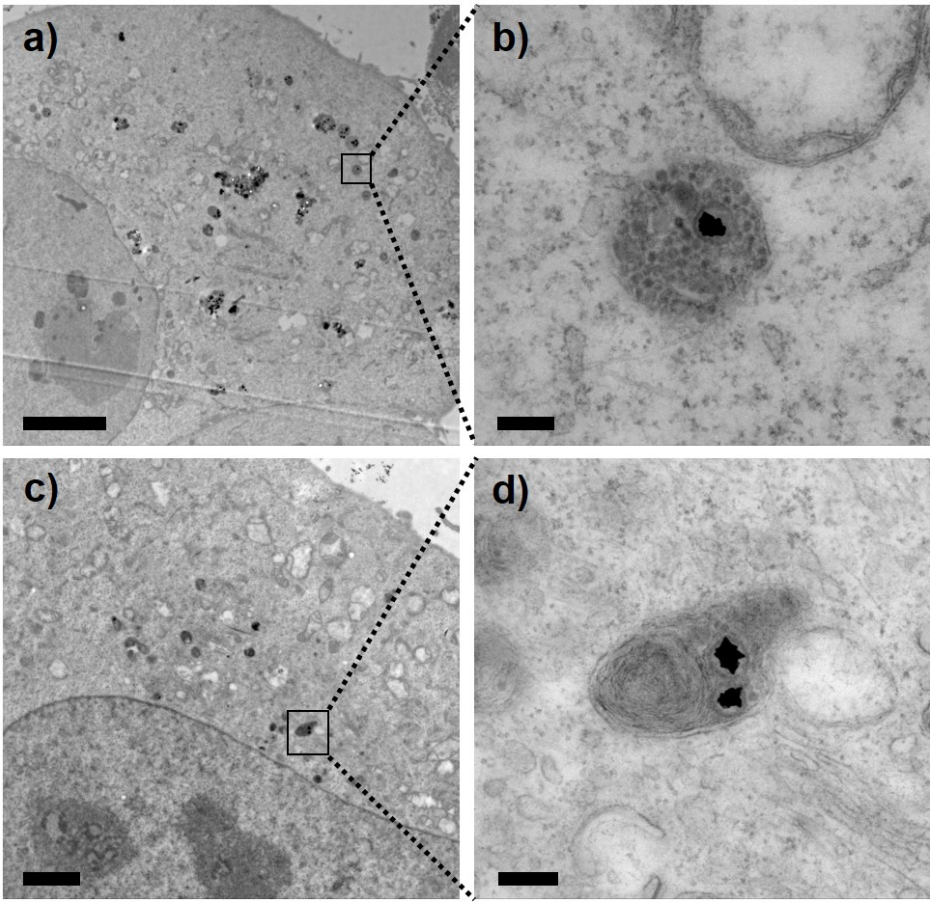

Figure S4. TEM images of HeLa cells after incubation with **N2** nanoparticles. Scale bars: (a) 5 µm, (c) 2 µm, (b,d) 200 nm.

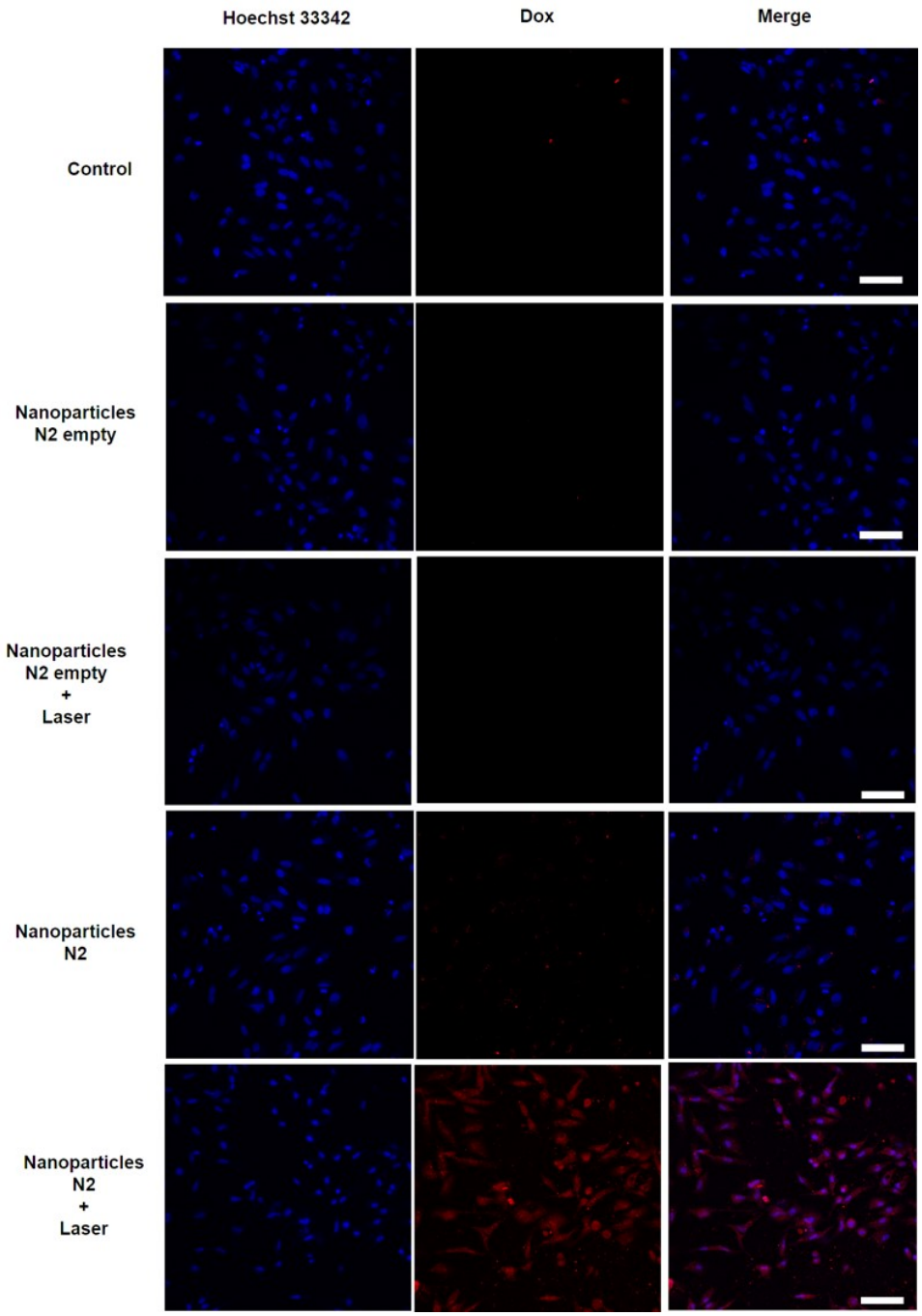

Figure S5. NIR light triggered release of Dox from **N2** nanoparticles in HeLa cells monitored by confocal laser scanning microscopy. From left to right: DNA marker (Hoechst 33342), doxorubicin (Dox) and combined (merge) fluorescence channels. From top to down: control cells (control), non-irradiated cells after incubation with nanoparticles (**N2 empty**) and NIR light irradiated cells after incubation with nanoparticles (**N2 empty** + Laser). non-irradiated cells after incubation with nanoparticles (**N2**) and NIR light irradiated cells after incubation with nanoparticles (**N2** + Laser). Scale bars: 100 μm.

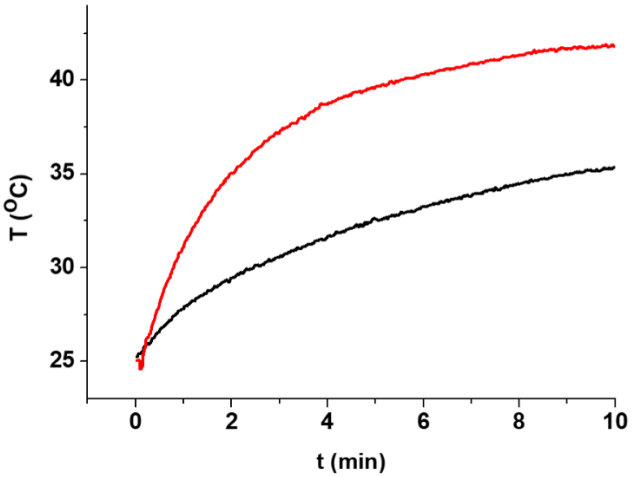

Figure S6. NIR light induced heating of bulk **N2** nanoparticle suspension at 100 µg mL^{-1} (red) and heating of control sample (**N2** nanoparticle suspension without irradiation) (black).

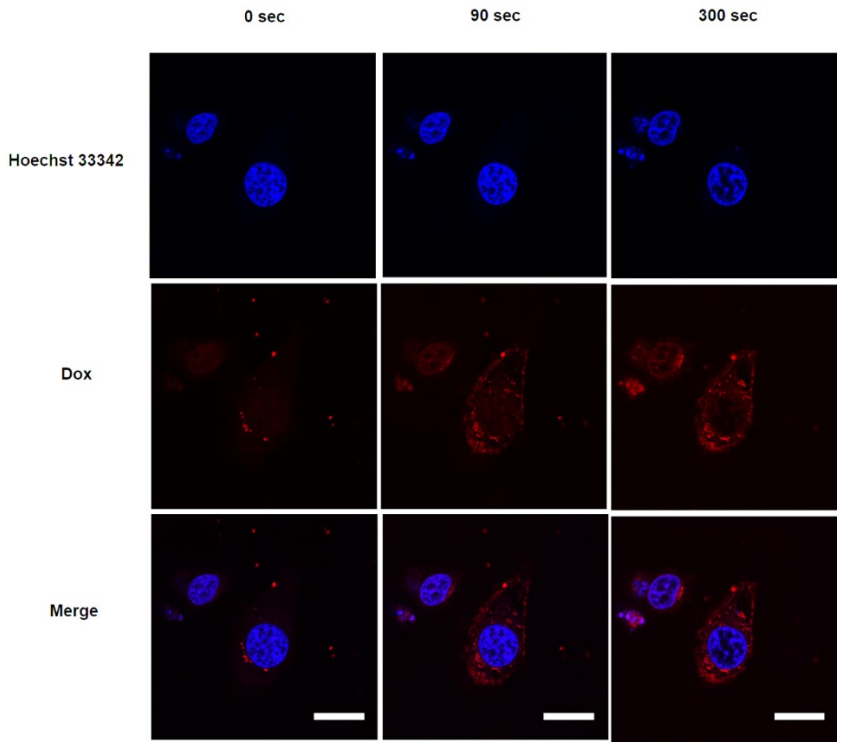

Figure S7. Release of Dox from **N2** nanoparticles in HeLa cells triggered by *in situ* irradiation at 633 nm using confocal laser scanning microscopy. From top to down: DNA marker (Hoechst 33342), doxorubicin (Dox) and combined (merge) fluorescence

channels. From left to right: before irradiation (0 sec), irradiation for 90 sec (90 sec) and after irradiation (300 sec). Scale bars: 20 μm.

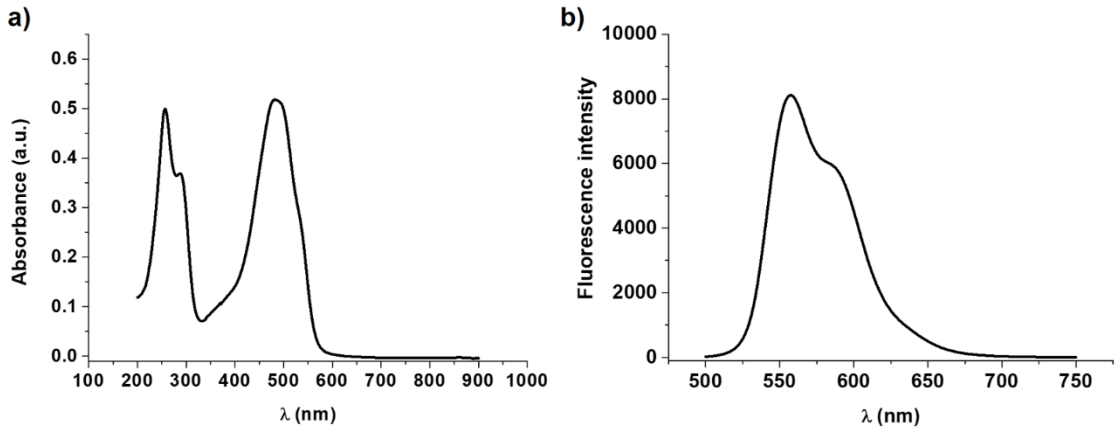

Figure S8. Optical extinction and fluorescence (λ_{exc} = 490 nm) spectra of Dox.

Discussion of the release mechanism

Although multi-photonic excitation of photolabile molecules requires the use of high laser powers due to the low multiphoton absorbing cross sections of chromophores[1-5], the strong electromagnetic field enhancement produced by localized surface plasmon resonance (LSPR) in gold nanoparticles[6,7] has been reported to facilitate multiphoton excitation of photolabile molecules even at low power irradiances.[8,9]

In principle, NIR light irradiation of gold nanoparticles can induce both thermal and photon-triggered molecular release. According to this, the photodissociation of 2-nitrobencil derivative can be produced upon irradiation of N2 nanoparticle, but a heating effect may also be produced with a possible thermal dissociation of PEG from the nanoparticle surface. However, we believe such heating effects during irradiation are less probable because the laser power used (below the intensities commonly employed for producing considerable photothermal effects). In fact, we conducted

additional experiments in which the temperature of N2 suspensions upon irradiation at 808 nm at 1 cm^{-2} was measured using a fiber-optic thermo-sensor (**Figure S6**). A temperature increase of the solution was observed reaching a plateau around 42 ºC after 10 min of irradiation at 1 W cm^2. These temperature values are relatively low and therefore, not expected to produce thermal decomposition of PEG from nanoparticle surface in large extension. Moreover, the intracellular release of Dox from **N2** nanoparticles was also triggered by *in situ* irradiation at 633 nm using the confocal laser scanning microscope (**Figure S7**). These results strongly suggested the Dox release in cells induced by NIR irradiation and attributed to a multiphotonic excitation of photolabile PEG onto nanoparticle surface. These results were similar to those reported by Voliani et all[8,9] using gold nanospheres and by our group using Janus nanoparticles.[10]

(1) Fomina, N.; McFearin, C.; Sermsakdi, M.; Edigin, O.; Almutairi, A. UV and Near-IR triggered release from polymeric nanoparticles. J. Am. Chem. Soc. 2010, 132, 9540–9542.

(2) Lin, Q.; Huang, Q.; Li, C.; Bao, C.; Liu, Z.; Li, F.; Zhu, L. Anticancer Drug Release from a Mesoporous Silica Based Nanophotocage Regulated by Either a One- or Two-Photon Process. J. Am. Chem. Soc. 2010, 132, 10645–10647.

(3) Aujard, I.; Benbrahim, C.; Gouget, M.; Ruel, O.; Baudin, J.-B.; Neveu, P.; Jullien, L. o-Nitrobenzyl photolabile protecting groups with red-shifted absorption: Syntheses and uncaging cross-sections for one- and two-photon excitation. Chem. Eur. J. 2006, 12, 6865 – 6879.

(4) Zhao, J.; Gover, T.D.; Muralidharan, S.; Auston, D. A.; Weinreich, D.; Kao, J. P. Y. Caged vanilloid ligands for activation of TRPV1 receptors by 1- and 2-photon excitation. Biochemistry 2006, 45, 4915-4926.

(5) Klán, P.; Šolomek, T.; Bochet, C. G.; Blanc, A.; Givens, R.; Rubina, M.; Popik, V.; Kostikov, A.; Wirz, J. Photoremovable Protecting Groups in Chemistry and Biology: Reaction Mechanisms and Efficacy. Chem. Rev. 2013, 113, 119−191.

(6) Hao, F.; Nehl, C. L.; Hafner, J. H.; Nordlander, P. Plasmon Resonances of a Gold Nanostar. Nano Lett. 2007, 7, 729-732.

(7) Jain, P. K.; El-Sayed, M. A. Plasmonic Coupling in Noble Metal Nanostructures. Chem. Phys. Lett 2010, 487, 153−164.

(8) Voliani, V.; Ricci, F.; Signore, G.; Nifosì, R.; Luin, S.; Beltram, F. Multiphoton Molecular Photorelease in Click-Chemistry-Functionalized Gold Nanoparticles. Small 2011, 7, 3271–3275.

(9) Voliani, V.; Signore, G.; Vittorio, O.; Faraci, P.; Luin, S.; Perez-Prieto, J.; Beltram, F. Cancer Phototherapy in Living Cells by Multiphoton Release of Doxorubicin from Gold Nanospheres. J. Mater. Chem. B 2013, 1, 4225–4230.

(10) Hernández Montoto, A.; Llopis-Lorente, A.; Gorbe, M.; Terrés, J. M.; Cao-Milán, R.; Díaz de Greñu, B.; Alfonso, M.; Ibáñez, J.; Marcos, M.; Orzáez, M.; Villalonga, R.; Martínez-Máñez, R.; Sancenón, F. Janus Gold Nanostars–Mesoporous Silica Nanoparticles for NIR-Light-Triggered Drug Delivery. Chem. Eur. J. 2019, 25, 8471.

FT-IR spectroscopy

Compound **1**

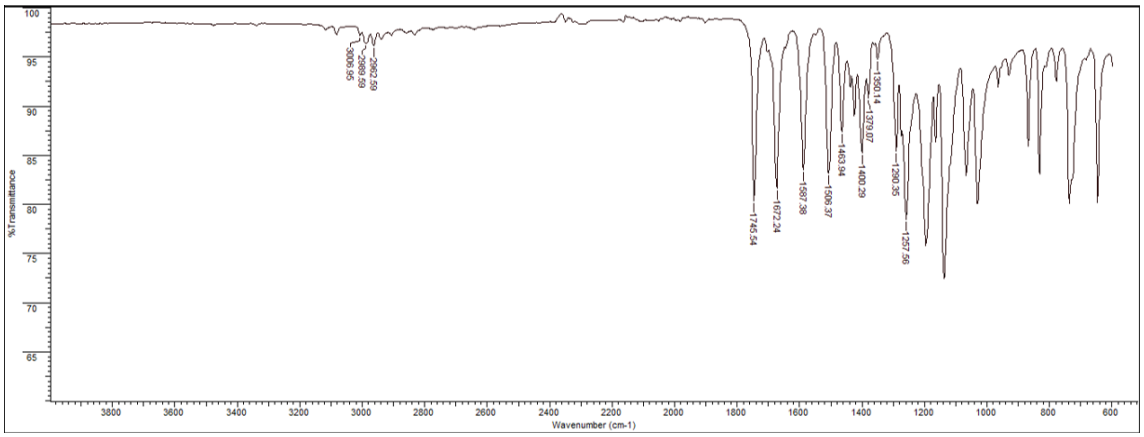

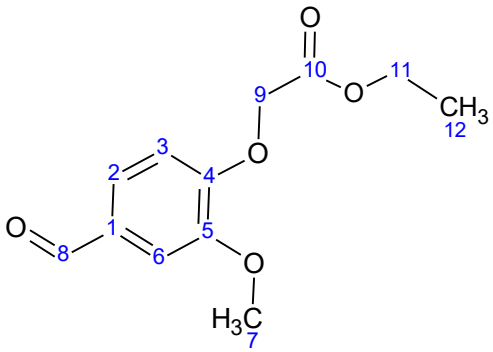

$\bar{\nu}$ (cm^{-1})	Molecular vibrations
3006	ν C_{sp2}-H
2989, 2962	ν C_{sp3}-H
1745	ν C=O (RCOOR)
1672	ν C=O (ArCHO)
1587, 1506, 1400	ν C⁼⁼C (Ar)
1463	δ C_{sp3}-H
1257, 1120	ν C-O (RCOOR)

Compound **2**

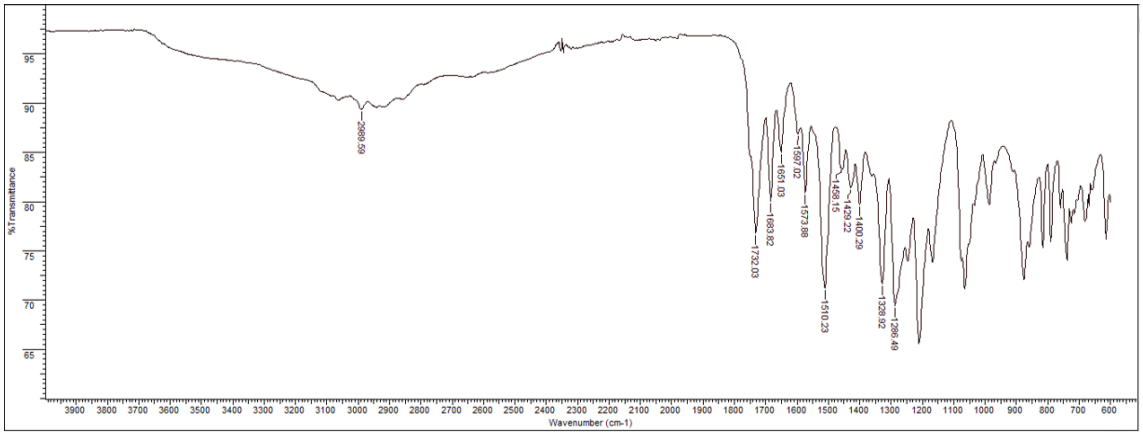

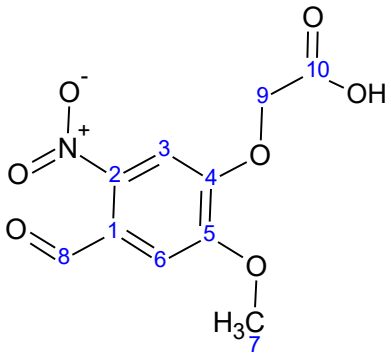

$\bar{\nu}$ (cm^{-1})	Molecular vibrations
3000	ν O-H (RCOOH)
1732	ν C=O (RCOOH)
1683	ν C=O (ArCHO)
1573, 1458, 1400	ν C⁼⁼C (Ar)
1510, 1328	$\nu_{as,s}$ N⁼⁼O (NO_2)
1200, 1050	ν C-O (RCOOH)

Compound **3**

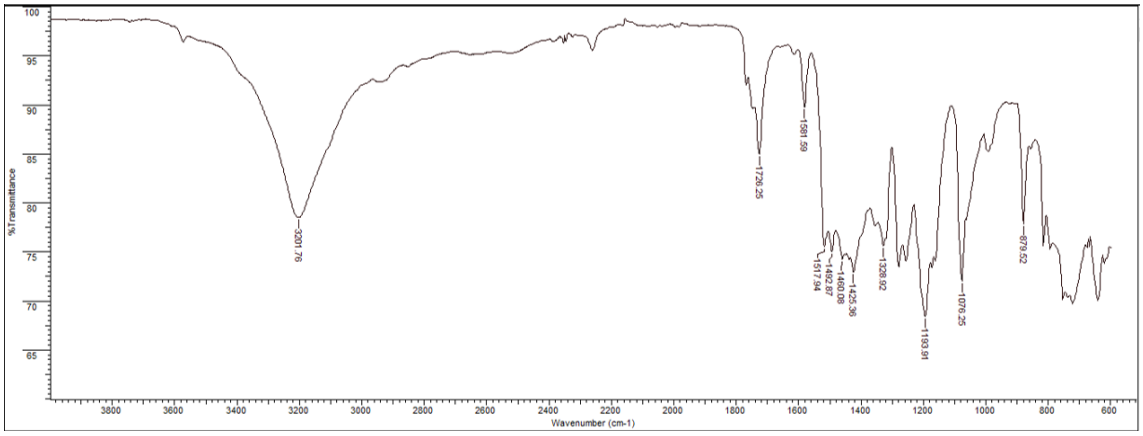

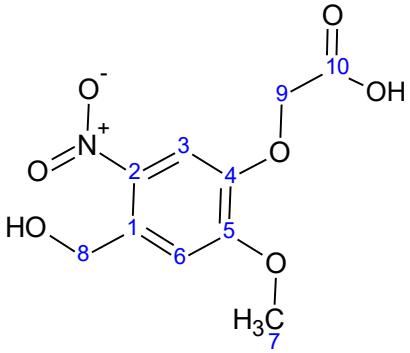

$\bar{\nu}$ (cm^{-1})	Molecular vibrations
3201	ν O-H ($ArCH_2OH$)
1726	ν C=O (RCOOH)
1581, 1492, 1425	ν C⁼⁼C (Ar)
1517, 1328	$\nu_{as,s}$ N⁼⁼O (NO_2)
1193, 1076	ν C-O (RCOOH)

Compound **5**

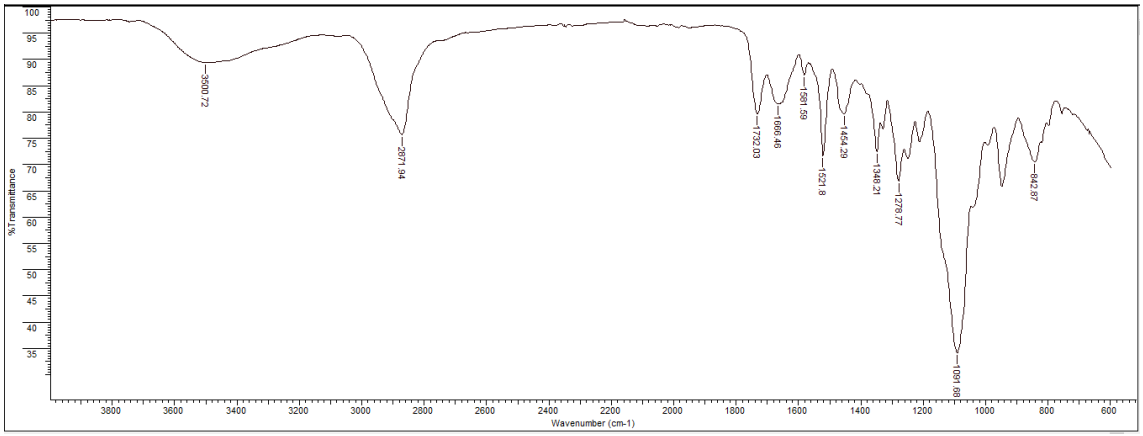

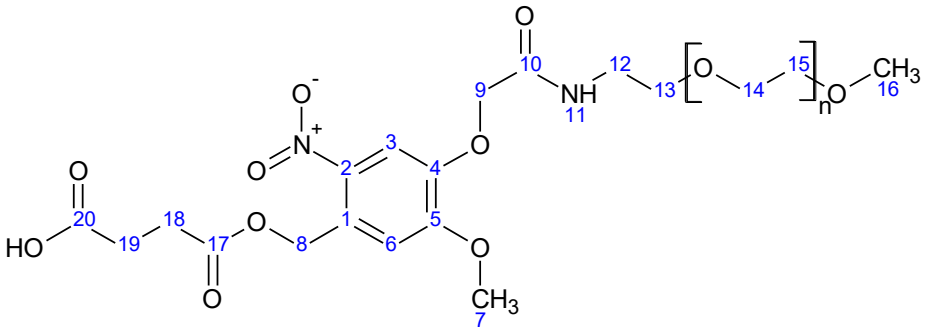

$\bar{\nu}$ (cm^{-1})	Molecular vibrations
3500	ν N-H (RCONHR)
3000	ν O-H (RCOOH)
2871	ν C_{sp3}-H
1732	ν C=O (RCOOH)
1666	ν C=O (RCONHR)
1581, 1454	ν C⎓C (Ar)
1521, 1348	ν $_{as,s}$ N⎓O (NO_2)
1278	ν C-O (RCOOH)
1091	ν C-O $(CH_2CH_2O)_n$

NMR spectroscopy

Compound **1**

^{1}H-NMR spectrum

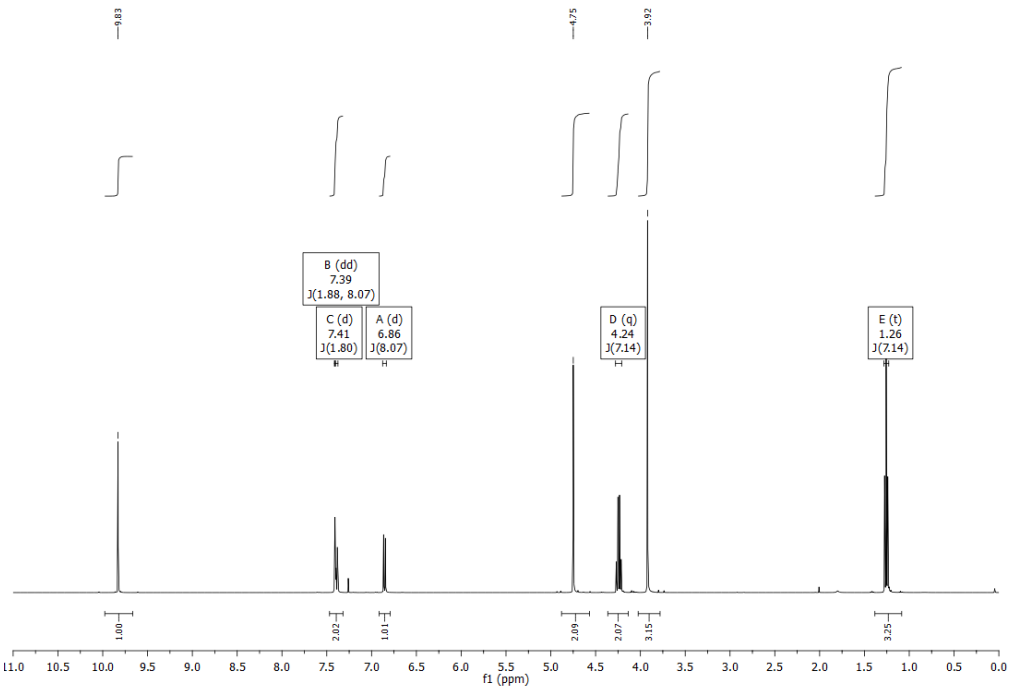

^{13}C-NMR spectrum

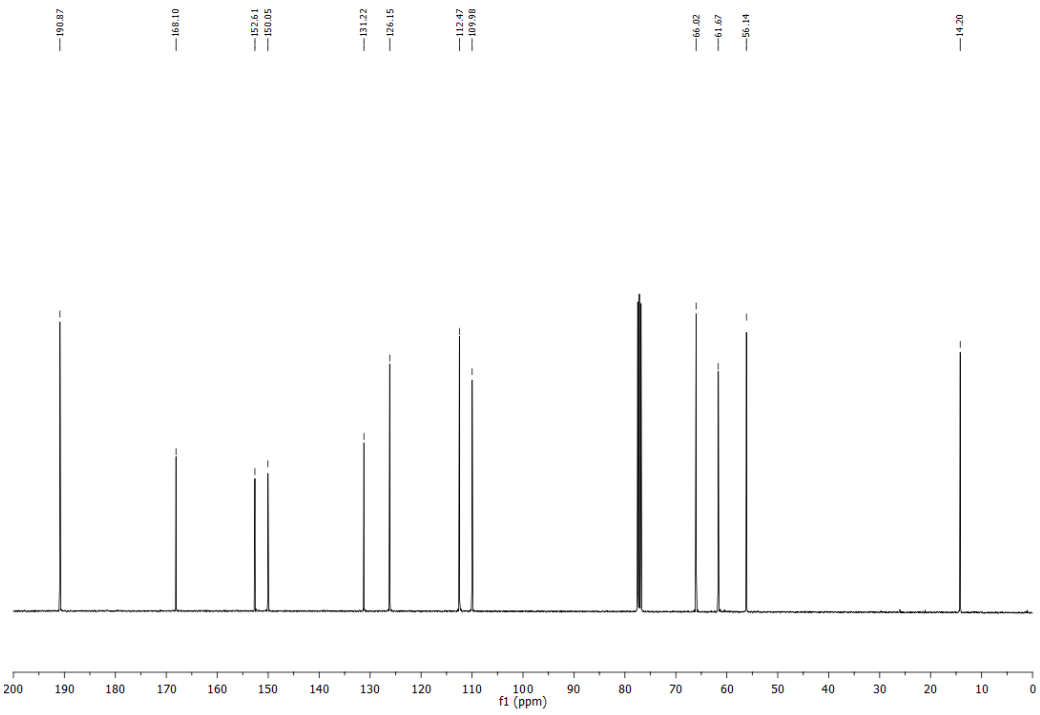

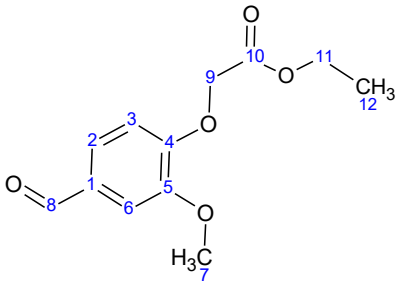

Chemical shift δ ^{1}H (ppm)	Integration	Multiplicity J (Hz)	Atom number
9.83	1	s	8
7.41	1	d (1.80)	6
7.39	1	dd (8.07; 1.88)	2
6.86	1	d (8.07)	3
4.75	2	s	9
4.24	2	q (7.14)	11
3.92	3	s	7
1.26	3	t (7.14)	12

Chemical shift δ ^{13}C (ppm)	Atom number

190.87	8
168.10	10
152.61	4
150.05	5
131.22	1
126.15	2
112.47	3
109.98	6
66.02	9
61.67	11
56.14	7
14.20	12

Compound **2**

^{1}H-NMR spectrum

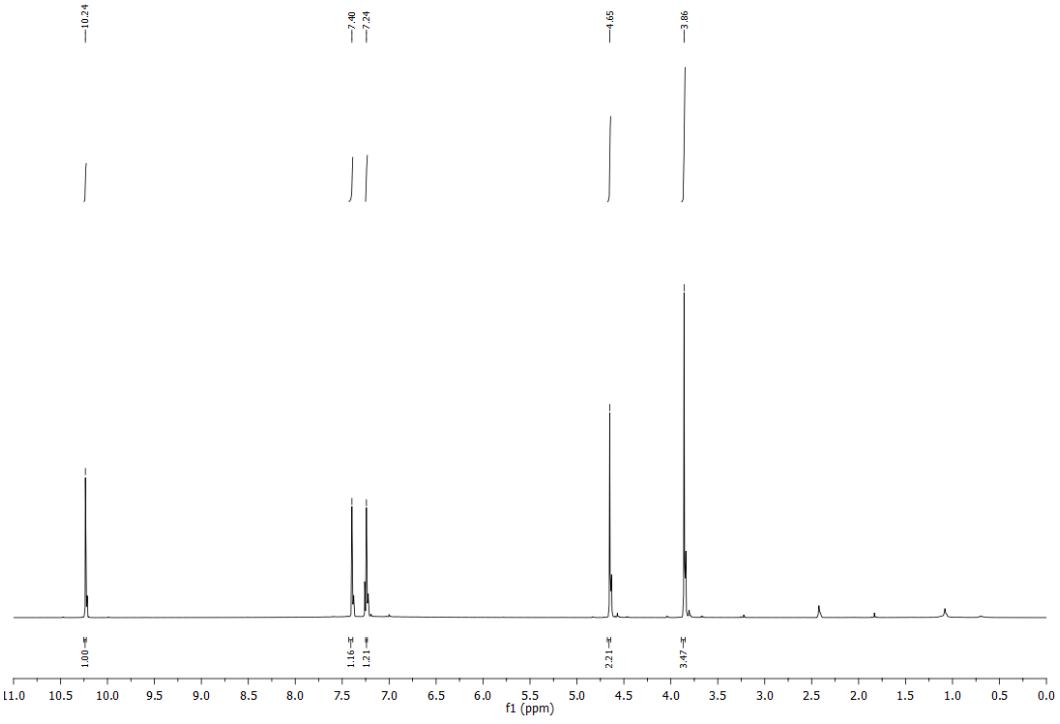

^{13}C-NMR spectrum

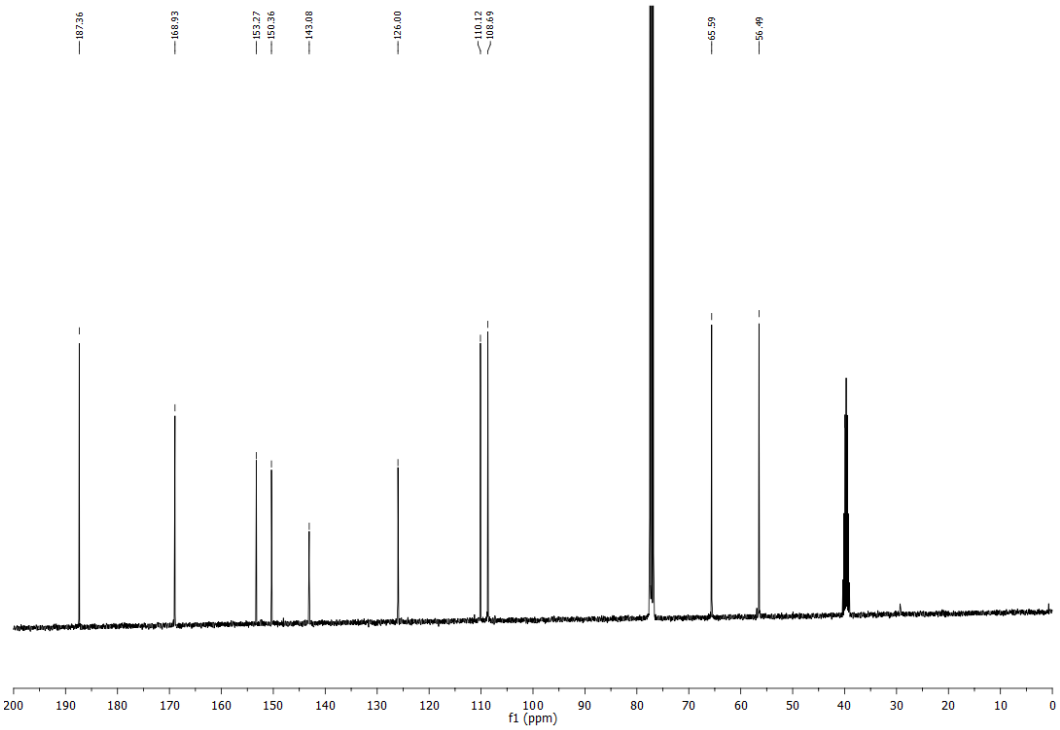

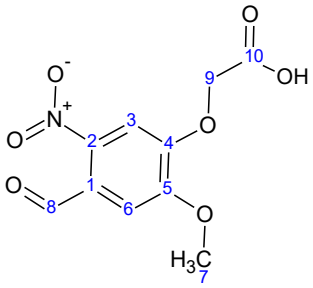

Chemical shift δ ^{1}H (ppm)	Integration	Multiplicity J (Hz)	Atom number
10.24	1	s	8
7.40	1	s	3
7.24	1	s	6
4.65	2	s	9
3.86	3	s	7

Chemical shift δ ^{13}C (ppm)	Atom number
187.36	8
168.93	10
153.27	5

150.36	4
143.08	2
126.00	1
110.12	6
108.69	3
65.59	9
56.49	7

Compound **3**

^{1}H-NMR spectrum

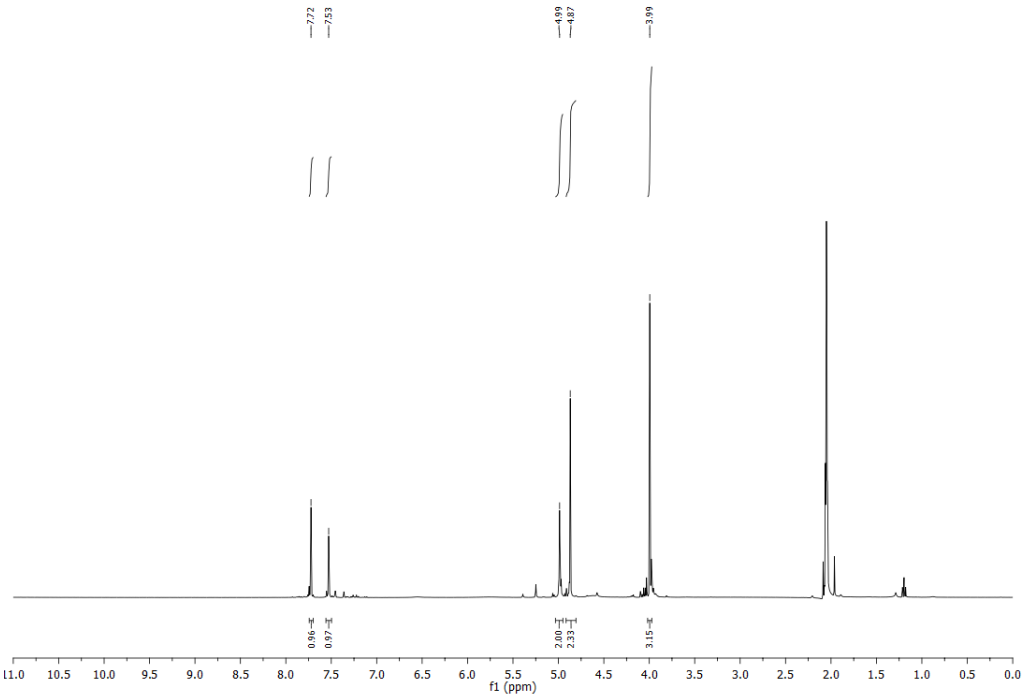

HSQC spectrum

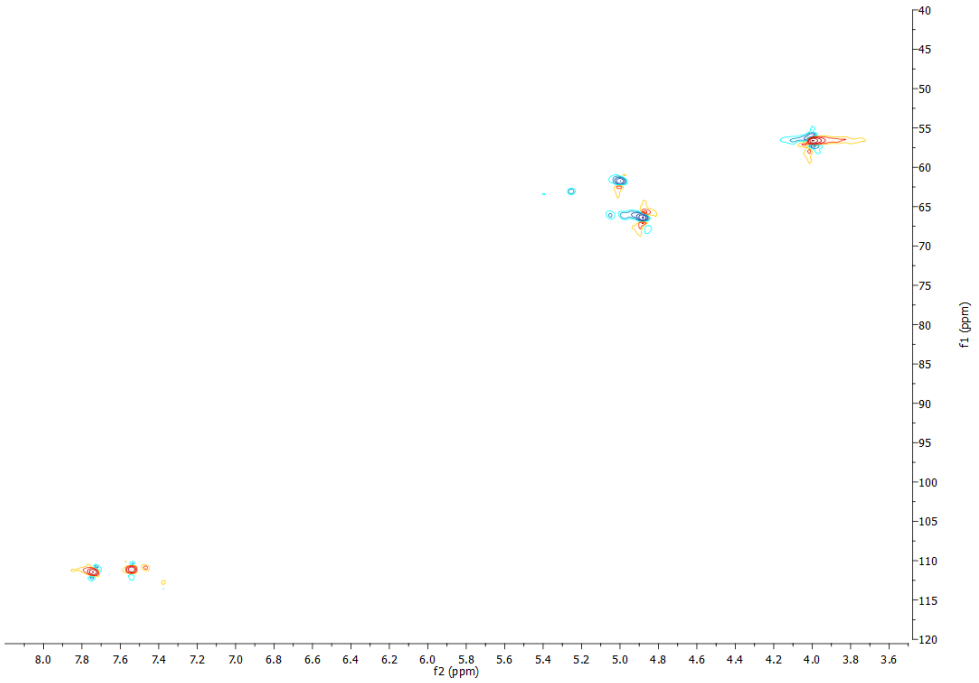

HMBC spectrum

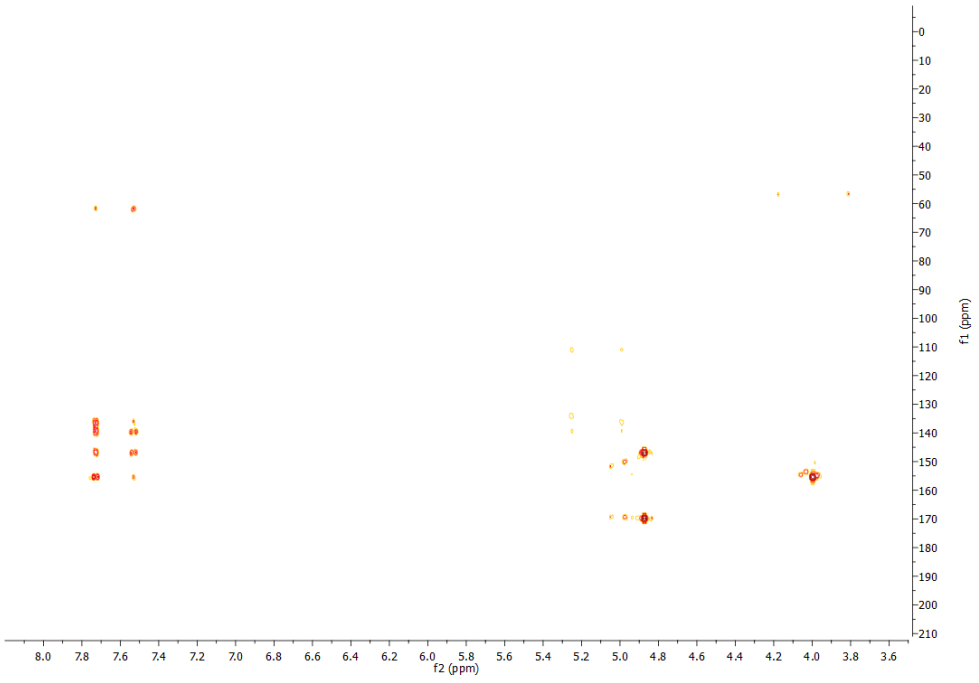

^{13}C-NMR spectrum

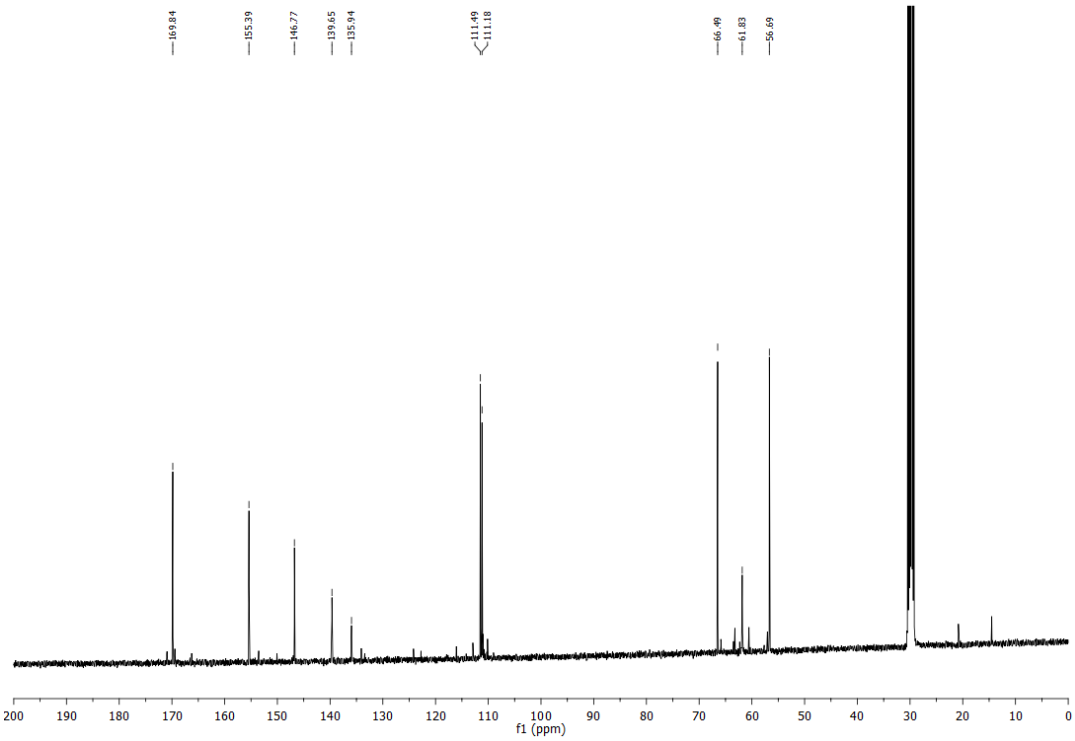

DEPT-135 spectrum

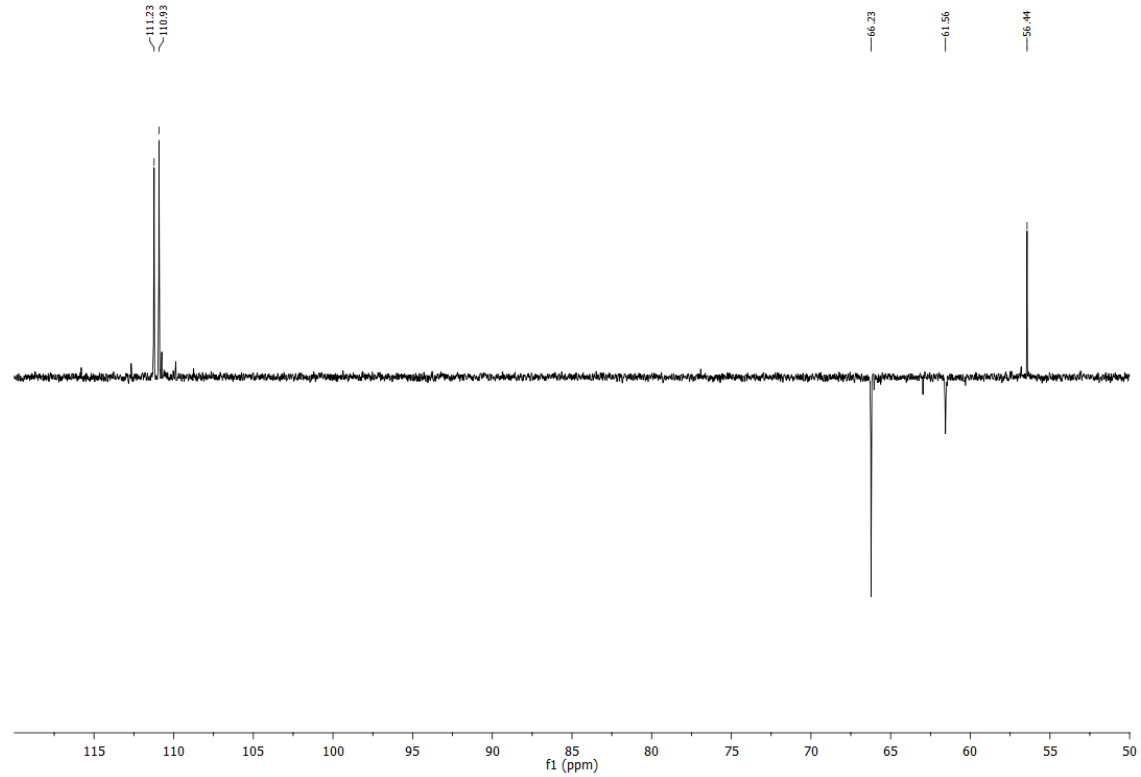

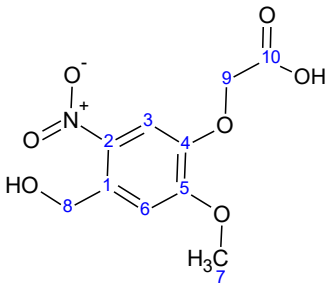

Chemical shift δ ^{1}H (ppm)	Integration	Multiplicity J (Hz)	Chemical shift δ ^{13}C (ppm) HSQC	Chemical shift δ ^{13}C (ppm) HMBC	Atom number
7.72	1	s	111.49	155.39, 146.77, 139.65, 135.94, 61.83	3
7.53	1	s	111.18	155.39, 146.77, 139.65, 135.94, 61.83	6
4.99	2	s	61.83		8
4.87	2	s	66.49	169.84, 146.77	9
3.99	3	s	56.69	155.39	7

Chemical shift δ ^{13}C (ppm)	DEPT-135 signal sign	Atom number
169.84		10
155.39		5
146.77		4
139.65		2
135.94		1
111.49	+	3
111.18	+	6
66.49	-	9
61.83	-	8
56.69	+	7

Compound **4**

^{1}H-NMR spectrum

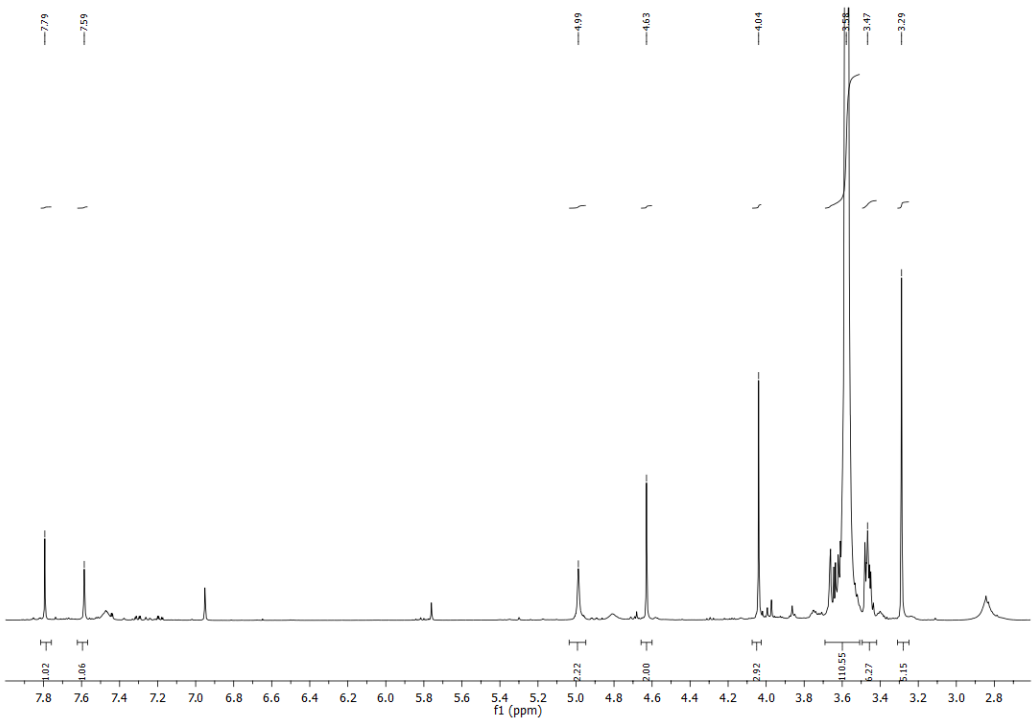

^{13}C-NMR spectrum

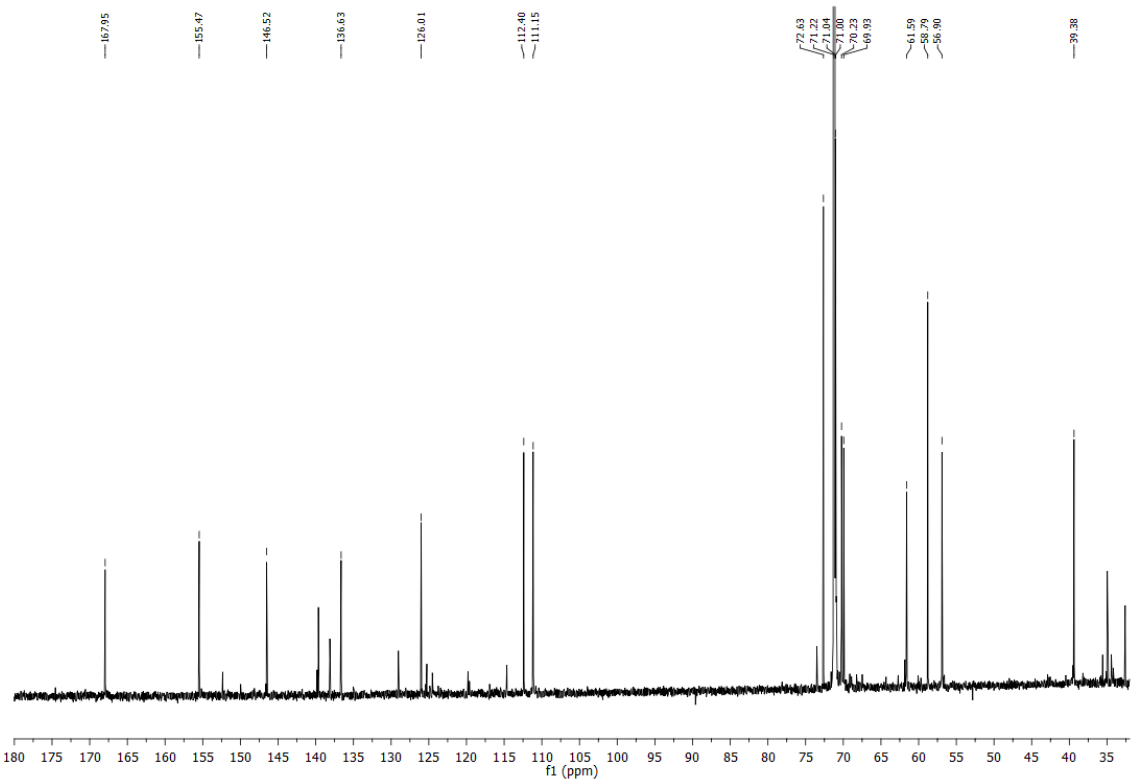

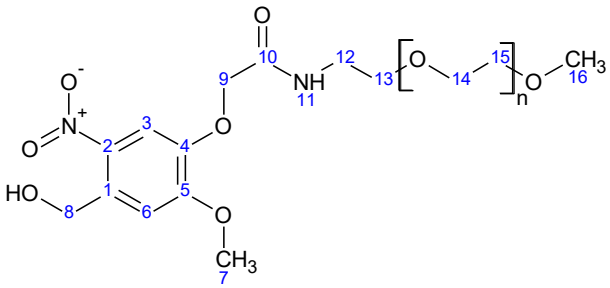

Chemical shift δ ^{1}H (ppm)	Integration	Multiplicity J (Hz)	Atom number
7.79	1	s	3
7.59	1	s	6
4.99	2	s	8
4.63	2	s	9
4.04	3	s	7
3.58	64	m	14,15
3.47	4	m	12, 13
3.29	3	s	16

Chemical shift δ ^{13}C (ppm)	Atom number
167.95	10
155.47	5
146.52	4
136.63	2
126.01	1
112.40	3
111.15	6
72.63	14
71.22	15
70.23	13
69.93	9
61.59	8
58.79	16
56.90	7
39.38	12

Compound **5**

^{1}H-NMR spectrum

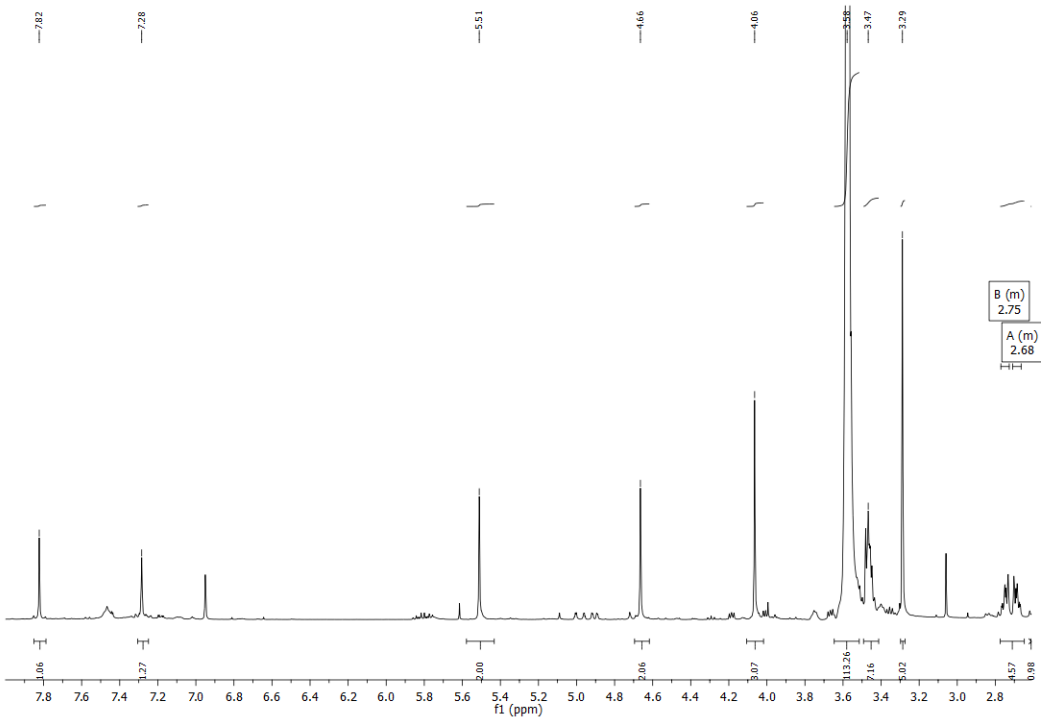

^{13}C-NMR spectrum

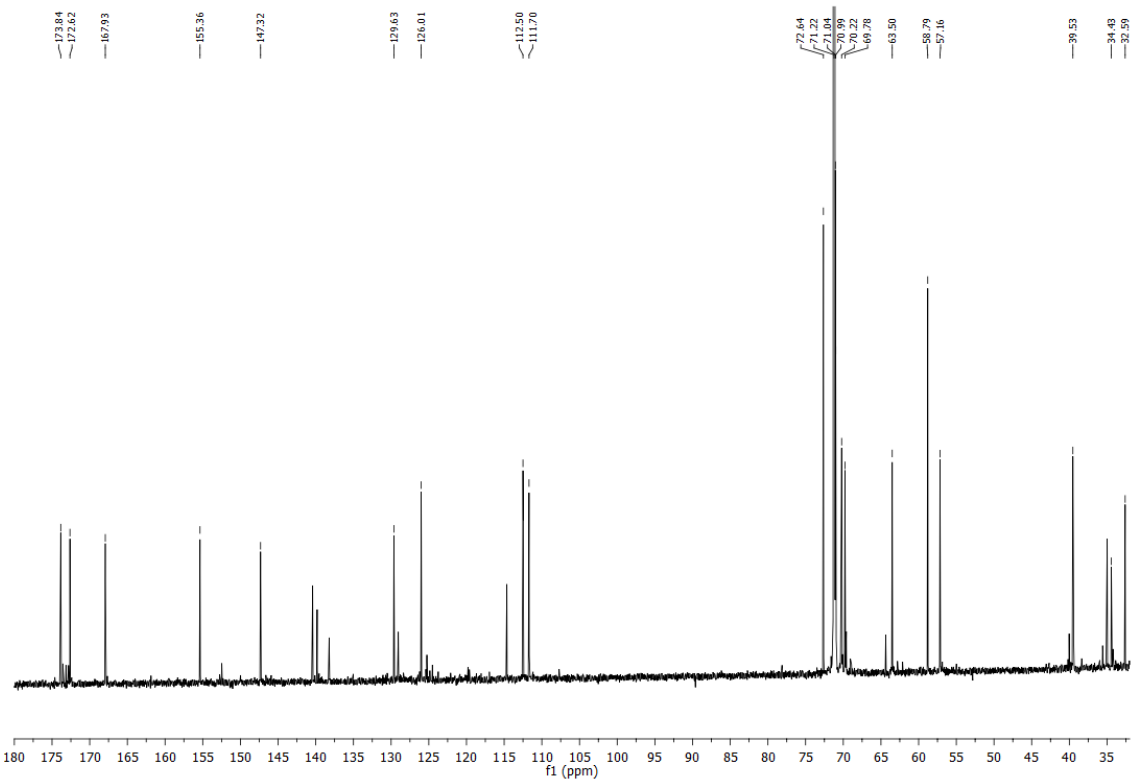

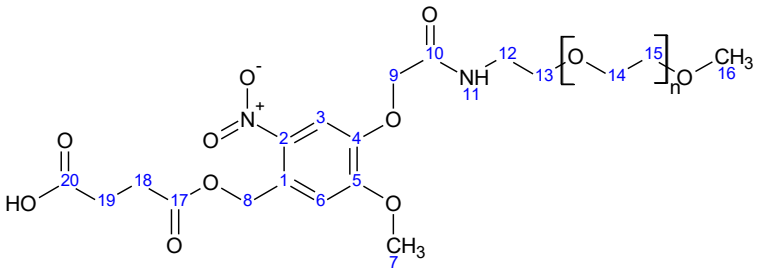

Chemical shift δ ^{1}H (ppm)	Integration	Multiplicity J (Hz)	Atom number
7.82	1	s	3
7.28	1	s	6
5.51	2	s	8
4.66	2	s	9
4.06	3	s	7
3.58	64	m	14,15
3.47	4	m	12,13
3.29	3	s	16
2.75	2	m	18

2.68	2	m	19

Chemical shift δ ^{13}C (ppm)	Atom number
173.84	17
172.62	20
167.93	10
155.36	5
147.32	4
129.63	2
126.01	1
112.50	3
111.70	6
72.64	14
71.22	15
70.22	13
69.78	9
63.50	8
58.79	16
57.16	7
39.53	12
34.43	18
32.59	19